Northumbria Research Link

Capacitive and resistive response of humidity sensors based on graphene decorated by PMMA and silver nanoparticles

Ishrat Rahim[1], Mutabar Shah[1], Afzal khan[1], Jingting Luo[2, *], Aihua Zhong[2], Min Li[2], Rashid Ahmed[3,**] Honglang Li[4] , Qiuping Wei[5] , Yongqing, Fu[6]

[1]Department of Physics, University of Peshawar, 25000 Peshawar Pakistan

[2]Shenzhen Key Laboratory of Advanced Thin Films and Applications, College of Physics and Energy, Shenzhen University, 518060 Shenzhen, China

[3]Department of Physics, Faculty of Science, Universiti Teknologi Malaysia, UTM Skudai, 81310 Johor, Malaysia

[4]Institute of Acoustics, Chinese Academy of Sciences, 100190, Beijing, China

[5]School of Materials Science and Engineering, State Key Laboratory of Powder Metallurgy, Central South University, Changsha 410083, China

[6]Faculty of Engineering and Environment, Northumbria University, Newcastle upon Tyne, NE1 8ST, UK

Corresponding authors: [*]luojt@szu.edu.cn (Jingting Luo)

[**]rashidahmed@utm.my (Rashid Ahmed)

Abstract

In this paper, we reported comparative study of the humidity characteristics of graphene/silver nanoparticles composite (Gr-AgNps) and graphene/silver nanoparticles/PMMA composite (Gr-AgNps-PMMA) based efficient humidity sensors. Aqueous solution of Gr-AgNps and Gr-AgNps-PMMA was drop casted over interdigitated copper electrodes with 50 µm gap embedded in the substrates in dust free environment. The band gap obtained from the UV-vis spectra for Gr-AgNps and Gr-AgNps-PMMA based humidity sensors was 4.7 and 4.1 eV respectively. The capacitive and resistive humidity response was studied using LCR meter (GW Instek817). Apparent increase in capacitance was observed (100-10,000 nF) with the increase in the humidity percentage (30-95 %RH) at lower frequencies for both the sensors. Resistance of the sensors dropped to zero as the humidity level is increased from 30 to 95 %RH in the chamber. The devices were tested for real time stability and for fast response/recovery time. Both the devices showed an excellent stability and response by recording their resistance and capacitance respectively. A lagging of RH decreasing response from RH increasing response was observed at 500 Hz frequency for both the sensors depicted from the hysteresis curve. The humidity response of Gr-AgNps was comparatively better than that of the Gr-AgNps-PMMA based humidity sensors.

Keywords: Humidity sensors, graphene, thin film, response/recovery, band gap

1. Introduction:

Reliable, portable and cost effective humidity sensors plays an important part in the prediction of floods, preserving and processing of foodstuffs, plants protection, maintaining the optimum conditions in manufacturing processes especially in electronic industries and weather telemetry applications [1, 2]. Currently, there is an extensive demand for efficient multifunctional sensors exhibiting debatable qualities such as long term physical and chemical stability, durability, fast response and recovery timing and cost affectivity [3-6]. Recently considerable attention has been directed toward the development of humidity sensitive materials or elements, especially nanomaterials due to their high surface to volume ratio including silicon [7], ceramic Nano-materials [8], semiconductor Nano-particles [9], metal oxide Nano-wires [10], Nano-films [11] and nanodots [12]. However, developing a novel humidity sensing material that possesses high and even sensitivity for the full range of humidity remains a challenge.

Graphene, a two-dimensional monolayer of sp^2-bonded carbon atoms exhibiting exceptional mechanical, thermal, and electrical properties, holds great potential for ultrasensitive detection [13]. Graphene was obtained using different physical and chemical procedures but initially it was prepared by micromechanical cleavage of graphite but due to lack of control over number of layers and inefficient processes for large scale production, this method fails on its behalf [19-20]. On the other hand, chemical vapor deposition and epitaxial growth procedures are inadequate due to high temperature processing and ultra-high vacuum requirements [14]. An alternative approach to cost-effectively produce graphene-based devices is to first produce graphene oxide (GO) and then reduce it to obtain graphene for device applications [15].

Hydrophobic nature of pure graphene limits its application in humidity sensors; however, functionalized graphene is hydrophilic showing promising results in vapour sensing [16]. Sensitivity of pure graphene humidity sensors was studied by Zakaryan *et al*. [17], and it was observed that with increasing the vapour concentration in the air opens up the band gap in the surface. Single layer graphene sensors were observed more sensitive to humidity as compared to two-layer graphene sensors. Breaking of the lattice structure and charge transfer due to HUMO/LUMO was responsible for the production of band gap in pure graphene layers [17]. Guo *et al.* [18] reported graphene oxide (RGO) thin film based humidity sensors by controlling the oxygen functional group concentration using laser tuning during the device fabrication. It was observed that functionalizing graphene with polymers increased the

efficiency of humidity sensors [18]. Yao *et al.* [19] investigated the stress based graphene oxide-silicon bi-layer humidity sensors. The sensor showed high humidity sensitivity, good repeatability, small humidity hysteresis and clear and fast response–recovery for a wide relative humidity range of 10–98 % RH. It has been reported that silver doping on oxides and ceramic materials has a positive effect on the efficiency of humidity sensors. Addition of optimum concentration of silver to the active materials enhances the dynamic range of the sensitivity of the sensors and reduce the response time up to four times comparative to undoped materials [20]. The increase in the silver concentration upto 3 wt% reduces the response /recovery time and increases the conductivity of the samples [21]. Hence silver nanoparticles can be proved to be virtuous additives for improving the humidity sensing mechanism. Similarly, polymers are encouraged for humidity sensing due to their high adsorption capabilities because water vapor molecules can easily pass through the pore openings present in these polymers surface [22]. Addition of silver nanoparticles and PMMA can be a better choice to improve the electrical properties of graphene for its application in humidity sensors [20].

In this paper, we present rapid response resistive/capacitive humidity sensing using drop casting technique for graphene nanocomposites. The humidity sensing properties of surface type graphene based thin films including sensitivity, response/recovery time were studied. A reliable, accurate and cheap humidity-sensing element for the measurement of relative humidity of the surrounding environment is developed in this study.

2. Experiment methodology

2.1. Materials

Fine powder natural graphite (99 wt%), potassium permanganate, sodium citrate (99 wt%), silver nitrate, sodium hydroxide, sodium borohydride and conventional MMA was purchased from sigma Aldrich. Hydrazine hydrate was supplied by Samchun Chem. Analytical grade organic solvents such as sulphuric acid (99 wt%), nitric acid and hydrogen peroxide (30 wt%) were used in this study without further purification. Glucose (dextrose) was purchased from Thermo Fisher Scientific.

2.2. Preparation of nanocomposites

Graphene oxide (GO) was obtained by the oxidation of natural graphite powder using the modified Hummer's scheme [23]. Graphene (Gr) was obtained by chemical reduction of the prepared GO powder using hydrazine hydrate as a reducing agent at 150 °C for 24 hours

by Rouff method. Graphene and silver nanoparticles (Gr-AgNps) composite was prepared according the following scheme. 0.5 g sodium citrate and 50 mg silver nitrate was added to the beaker containing a graphene solution (10 wt% dispersion in DMF) during ultrasonication. The solution was stirred until a homogenous suspension was obtained. Sodium borohydride ($NaBH_4$) was added to the mixture at 100 °C after 30 minutes, and the temperature was maintained for 8 hours. After filtration and drying of the obtained product, it was immersed in sulphuric acid to remove traces of sodium. The resulting solution was filtered, rinsed with distilled water and was finally dried in the oven. Gr-AgNps-PMMA nanocomposite was obtained via in situ polymerization. 100 mg graphene was added into 10 ml of MMA and the mixture was sonicated for 1 hour using W225R probe sonicator. 0.2 wt% AgNps solution was also added to the reaction mixture. The reaction was maintained at 60 °C for 8 hours until the mixture turned into transparent solid. The blend poured in 20.5 mm wide cylindrical mould for drying.

2.3. Sensor fabrication

Gr-AgNps and Gr-AgNps-PMMA nanocomposite solutions were drop casted on clean interdigitated copper electrodes with 50 µm gap and 1 mm width embedded in the substrates in dust free environment shown as in figure 1(a). The thickness of the electrodes was approximately 100 nm and thickness of the deposited film was about 300 nm measured by using thickness profilometer. Figure 1(b) shows the schematic diagram of the device fabricated for the present article. The fabricated sensor is 35 mm in length and 26 mm in width. The 5 to 6 pair of IDEs are deposited in 20 mm length of the device.
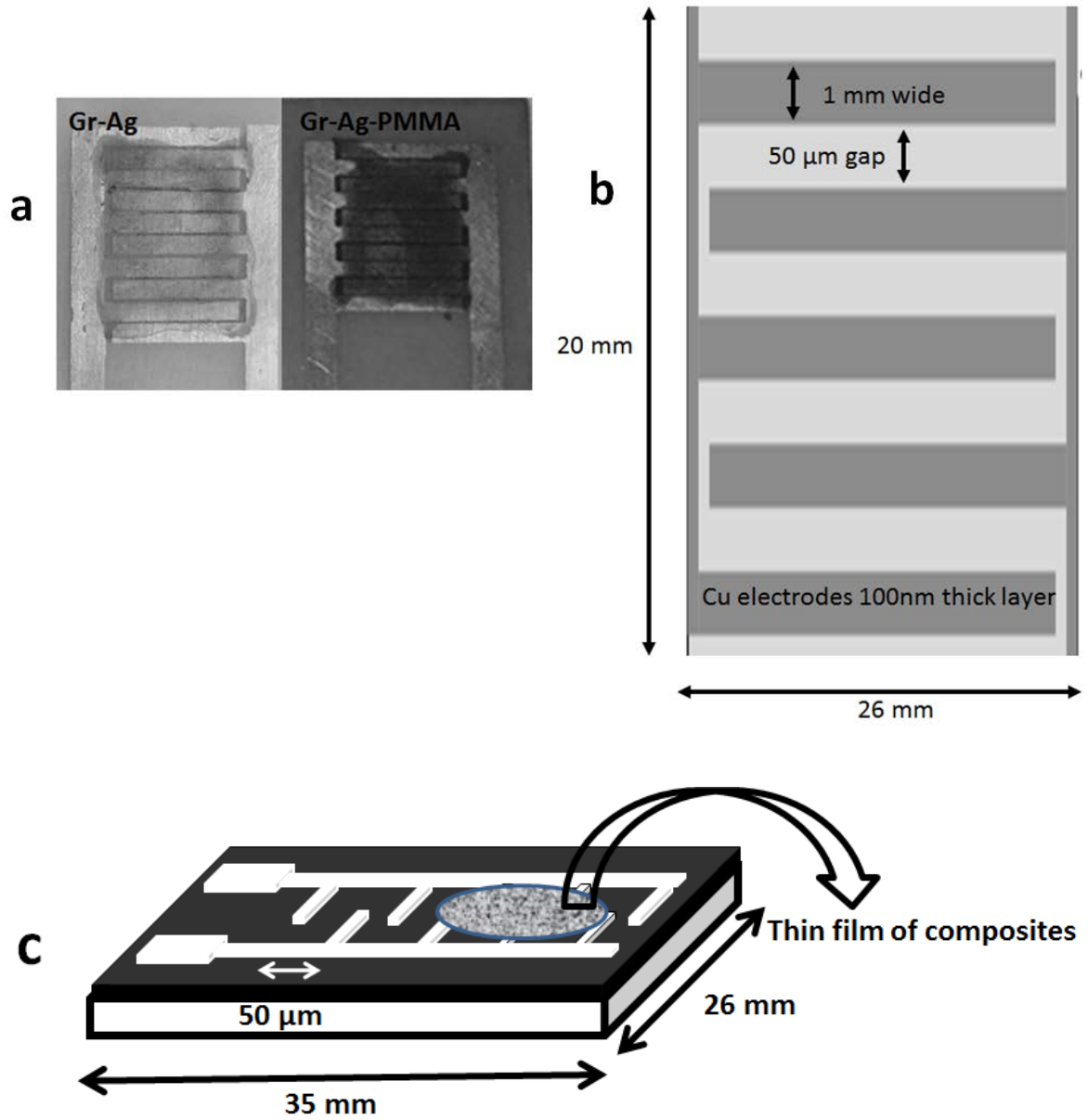
Figure 1: (a) image of the sensors (b) IDEs detailed structure (c) schematic figure of the sensor.

2.4. Setup for measuring sensing properties:

Humidity is the measure of water content present in the air. Relative humidity (RH) can be expressed as the ratio of partial pressure of moisture content to equilibrium vapour pressure at ambient temperature as RH= $\frac{p_s}{p_w}$ [24]. Digital hygrometer (RH 101) was used to measure humidity level and LCR meter (GW Instek817) was used to observe capacitance and resistance at different humidity level. The schematic of the experimental setup for recording the data of the sensors is shown in figure 2. Response time for capacitive/resistive sensor is

defined as the time taken by the sensor to absorb water vapours when the relative-humidity is increased rapidly and recovery time is the time taken by the sensor to recover itself to its initial state by desorbing water vapours with rapid decrease in humidity. The time, the sensor required to reach its final value before saturation, was recorded as the response time and vice versa for recovery time [25].
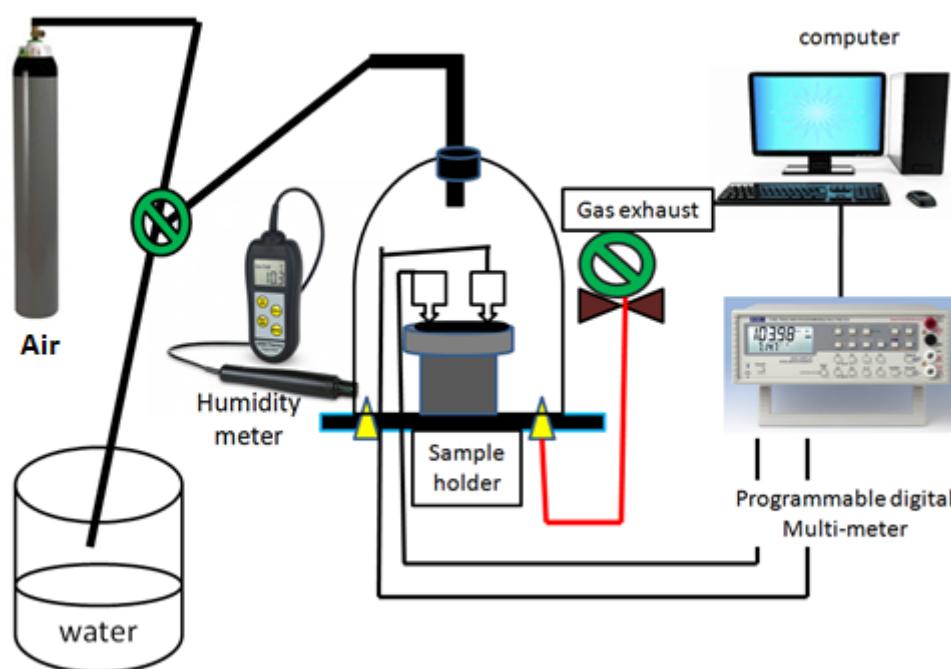

Figure 2: Schematic diagram of the experimental setup for humidity sensing.

30 kV Scanning Electron Microscope (JSM-5910, JEOL, Japan) was used to perform Scanning electron microscopy (SEM) of the thin films. To measure the optical UV Vis spectra of the prepared materials solution, Shimadzu UV-160A Lab UV/VIS Ultraviolet-Visible Recording Spectrophotometer was used.

2. Results and discussions

Figure 3(a, b & c) shows the scanning electron micrographs of the pure graphene and nanocomposites thin film. Sheet like structure of graphene is visible in figure 3(a). The transparency in the SEM image lead us to believe that the thin film consists of 5-6 layers of graphene which yields the thickness of the film to be roughly 50 nm. Clusters of silver nanoparticles are attached to the sheets which can be clearly seen in figure 3(b). we can see in

the SEM image that graphene sheets are thickly covered by the silver nanoparticles and the average size of Ag nanoparticles is about 10 nm. Figure 3(c) shows the surface morphology of Gr-Ag-PMMA nanocomposite. Addition of silver nanoparticles and PMMA distort and break the smooth stretched sheets of graphene making it rough and wrinkled. These voids in the film behave as a resting site for the moisture in the surrounding and hence increase the sensing abilities of the film.
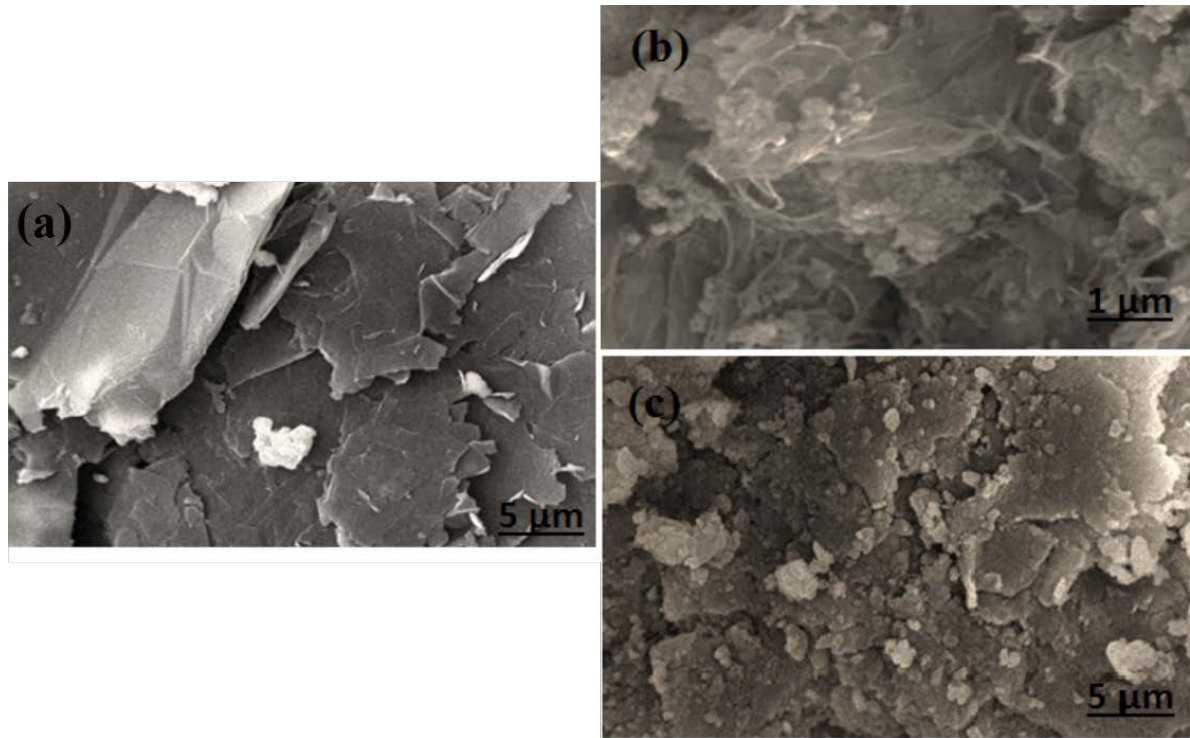

Figure 3: SEM micrographs of (a) Gr (b) Gr-AgNps (c) Gr-AgNps-PMMA thin film.

Figure 4 shows the UV-VIS analysis of the prepared solutions that are later being drop casted on the substrates that confirms the formation of these nanocomposites. The spectra show maximum absorbance in the visible and near ultraviolet (200-400 nm) region showing a high intensity peak for Gr-AgNPs nanocomposite. The band gap of the samples can be calculated using the wavelength and absorption coefficient from the UV-VIS spectra. The absorption coefficient α was calculated from the following equation.

$$\alpha = \frac{4\pi k}{\lambda} \tag{1}$$

Figure 5 shows the band gap of the thin film by tracing the linear portion of the graph plotted between $(\alpha h\upsilon)^2 \, eV^2 \, cm^{-2}$ and energy $(h\upsilon)$ eV. The band gap obtained for Gr-AgNps and Gr-AgNps-PMMA thin film was 4.7 and 4.1 eV respectively. It should be reminded that pure graphene is a zero-band gap material and the absorption peak of Gr-AgNps is mainly from Ag nanoparticles because of the plasma resonance properties of the nanoparticles metal. After the addition of PMMA, the plasma resonance properties of Ag nanoparticles become weaken, which reduces the hot carrier injection and the bandwidth shows red shift in Figure 4.
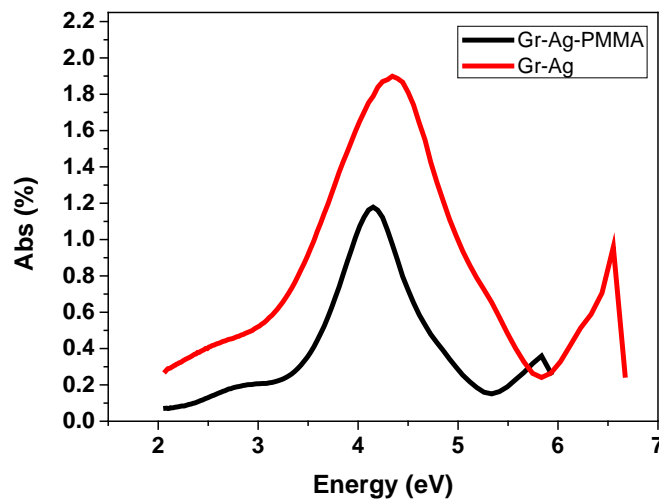

Figure 4: UV-VIS spectra of Gr-AgNps and Gr-AgNps-PMMA nanocomposites.
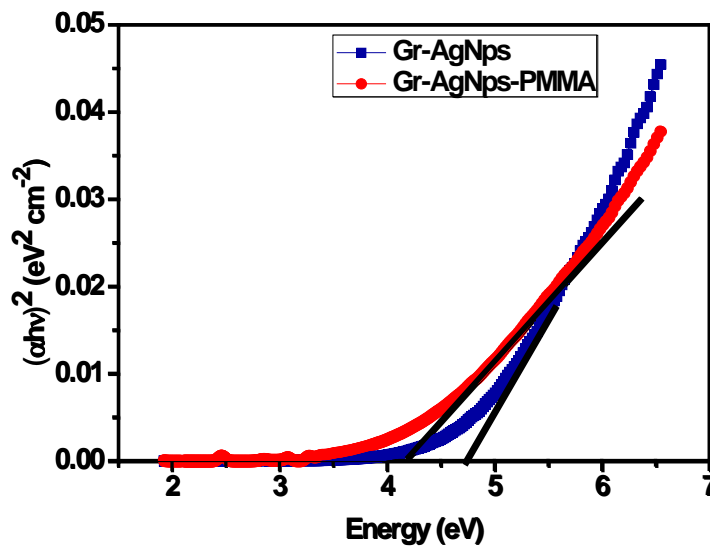

Figure 5: Band gap of Gr-AgNps and Gr-AgNps-PMMA nanocomposites.

The amount of water concentration irrespective of the surrounding temperatures is usually called as absolute humidity. The thin film of the material enclosed in two metal electrodes act as a tiny thin film capacitor and the material act as a dielectric. As per the capacitive technique for sensors is concerned, the capacitance of the material varies non-linearly with respect to the relative humidity in the chamber [26, 27]. The factors that affect the capacitance of the material in the sensor are polarization and dielectric permittivity constant of the sensing material, gap between the electrodes and electrode geometry [28]. Figure 6 (a) & 6 (b) displays the change in the capacitance of the thin film with the increase in humidity in the chamber for 30-100 %RH at five different frequencies adjusted in the LCR meter. A constant temperature of 300 K maintained in the test chamber while recording the values of capacitance with respect to the different humidity level. The values of the capacitance of the samples clearly increase with the increase of vapour concentration in the surrounding. It is important to note that the electrodes on the substrate can possibly take part in the sensing mechanism hence the copper interdigitated electrodes used in this study were exposed to the same humidity level before exposing the active materials. An error of 0.2 % has been subtracted from the recorded values of the capacitance for the sensors. The values of the capacitance of the samples clearly increase with the increase of vapour concentration in the surrounding. Moreover, slightly high increase has been noticed at lower input frequencies. Whenever the sensing material is exposed to moisture, the vapours settle down in the voids and spaces in the thin film surface. Since water has a high dielectric constant of round about 80, the diffusion of tiny water drops onto the thin film increases the dielectric constant consequently increasing the capacitance that can be inferred by knowing the direct relation between the dielectric constant and capacitance given by the equation 2 [29].

$$C = \frac{A \varepsilon_o \varepsilon_r}{d}$$
(2)

where A is the area of plate of a capacitor, ε_o is permittivity of free space, ε_r is relative permittivity of a material and d is a small separation between the plates. In comparison, Gr-AgNPs shows high capacitive variation with the change in humidity with maximum capacitance of 10000 nF as in figure 6(a) while Gr-AgNps-PMMA reach upto 8000 nF at 100 Hz frequency depicted in figure 6(b). The sensitivity of these sensors is effected by the concentration of the additives. Gr-AgNPs nanocomposite contains 0.5 wt% of AgNps, however, increasing the concentration of AgNps in the composite will increase the grain size

of the clusters which will boost the carrier transport in the films, thus increasing the sensitivity of the films with the absorption of water molecules [30]. PMMA itself is a polar molecule with dielectric constant lying between 3 and 7 which can be increased by elevated temperature annealing. The addition of the polymer to the nanocomposites lowers the dielectric constant which in return effect the conductivity of the nanocomposite thin film.
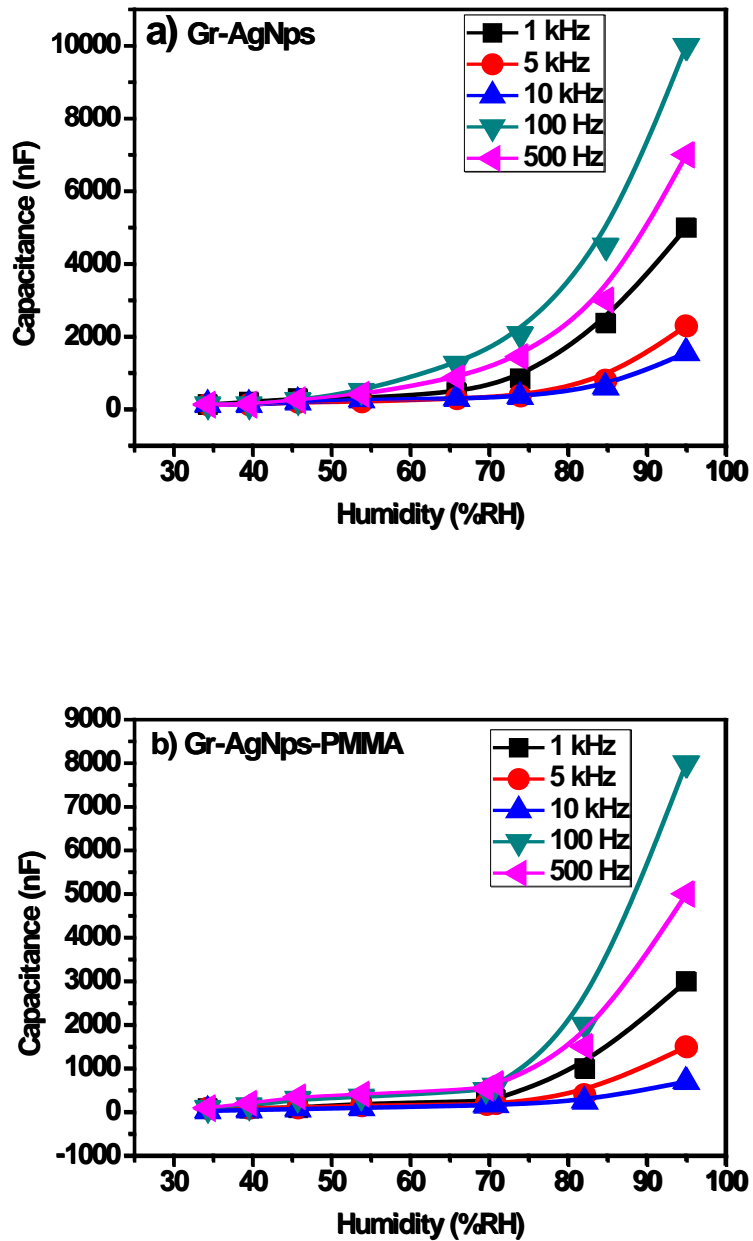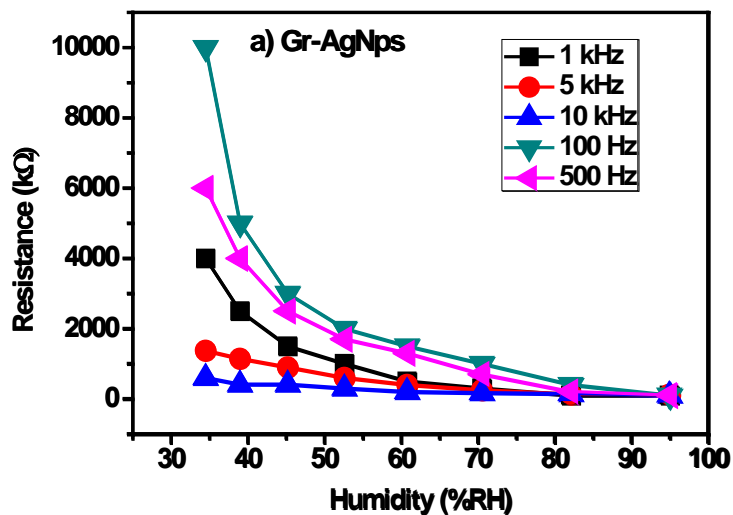

Figure 6: Variation of capacitance with different %RH at different frequencies for (a) Gr-AgNps(b) Gr-AgNps-PMMA surface type sensors at 300 K.

The resistive behaviour of the sensors was also satisfying shown in figure 7 With the adsorption of water, the conductivity of the film increases which causes the decrease in resistance with rise of humidity level. The electrical response of the sensor is due to proton hoping between the chemisorbed hydroxyl groups at lower RH values. So as the films reach the physiosorbed states, the resistance almost becomes zero due to increase in conductivity [31]. There is an abrupt decrease in resistance of the fabricated sensors in 35-50 %RH humidity levels. Further at higher humidity concentration the resistance eventually decreases to zero. The mechanism for increase in conduction due to water vapor adsorption on material surface is given by Grotthuss chain reaction [32]. It is evident from the plots that Gr-AgNps shows a better and dominant resistive response in figure 7 (a) as compared to Gr-AgNps-PMMA sensor shown in figure 7 (b). It can be noticed from the figure 7 (a) and 7 (b) that as the values of the applied frequency is lowered, the value of resistance of the sensor decreases. This effect can be attributed to Maxwell–Wagner–Debye relaxation [33]. Higher resistance values at lower frequency can also be better explained using the space charge polarization. At low applied frequencies, the change in net electric field is very small and it is easily followed by the polarized charges hence increasing the net resistance. However at higher frequencies, the polarization is unable to respond to the rapid variation in the applied electric field, reducing the resistance of the material to almost zero [34].
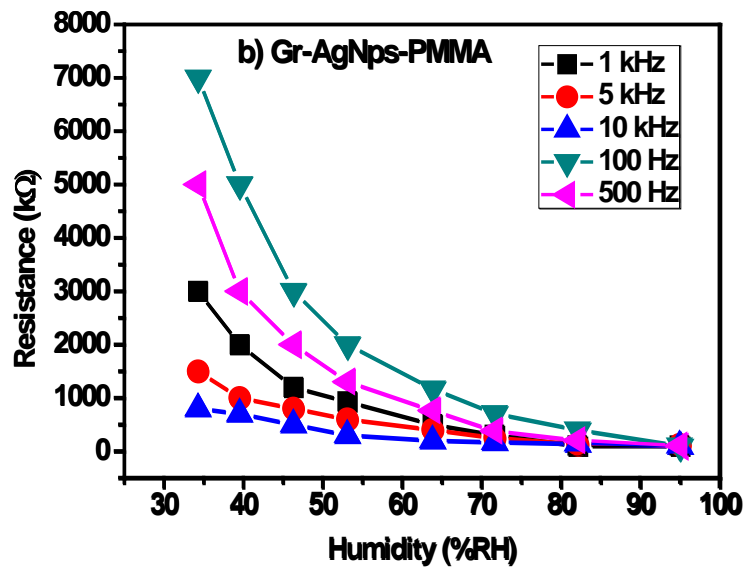
Figure 7: Resistance variation profiles with different %RH at different frequencies for (a) Gr-AgNps(b) Gr-AgNps-PMMA surface type sensors at 300 K.

Large scale applications of graphene based sensors are questioned over their stability by the industrialist and researchers. The stability of Gr-AgNps and Gr-AgNps-PMMA based surface type sensors were repeatedly tested by recording their resistance values at fixed humidity in a period of 30 days under strict temperature conditions. Figure 8(a) and 8(b) shows the profiles of the resistance variation with the passage of days for Gr-AgNps and Gr-AgNps-PMMA surface type sensors respectively at the temperature of ~300 K. The variation in resistance is less than 2% at each humidity region for one month at 100 Hz for both the sensors depicted clearly in the figure 8. It has been reported earlier that the surface type sensor shows better stability than sandwich type device structure therefore we opted surface type sensors to work with [35].
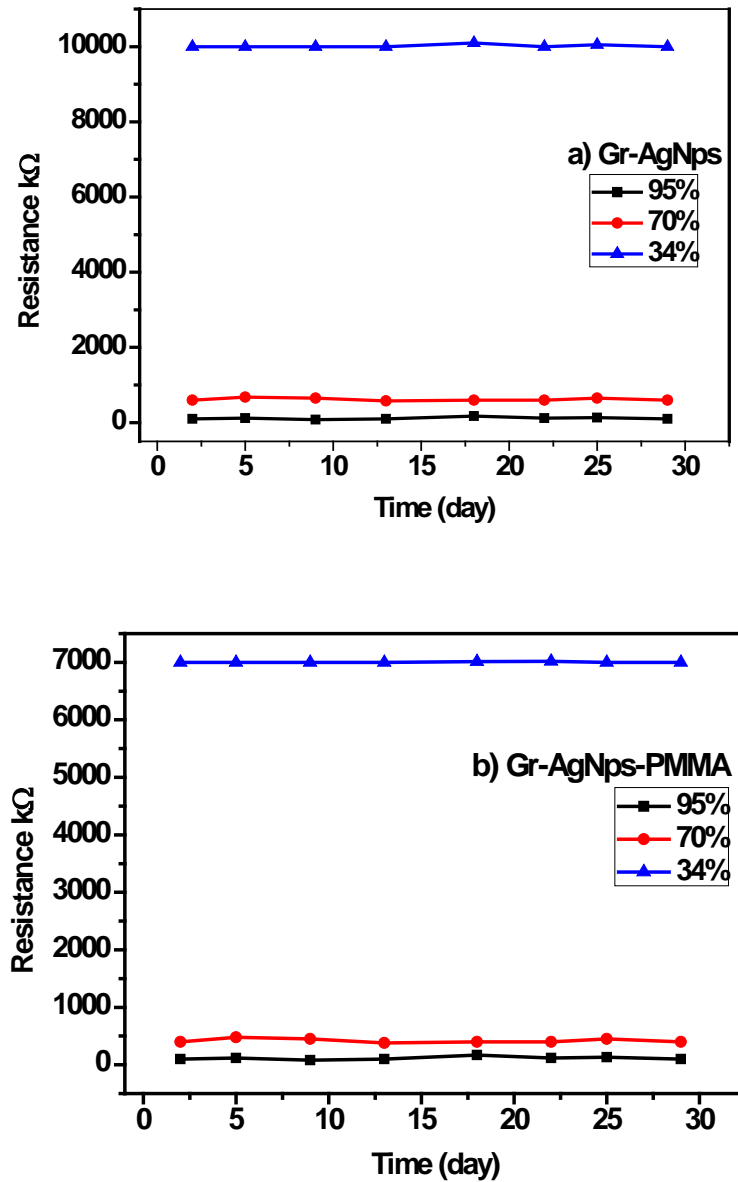
Figure 8: Variation of resistance with time at different % RH for 100 Hz frequency (a) Gr-AgNps(b) Gr-AgNps-PMMA surface type sensor <mark>at the temperature of ~300 K</mark>.

Figure 9 (a) portrays the sensors to have low response and recovery timings for capacitive variations <mark>at 300 K</mark>. The response time is 10 and 12 s for Gr-AgNps and Gr-AgNps-PMMA based surface type sensors respectively. The recovery time of both the sensors matched with each other having a common value of 9 s. Pure graphene sensors, however, are comparatively slower and less sensitive as compared to the nanocomposite based humidity sensors as depicted in figure 9 (a) and 9 (b) represented as "Gr". Moreover, these calculated values for

the three sensors are small as compared to the values reported in the literature as far as graphene based sensors are concerned [13, 36].
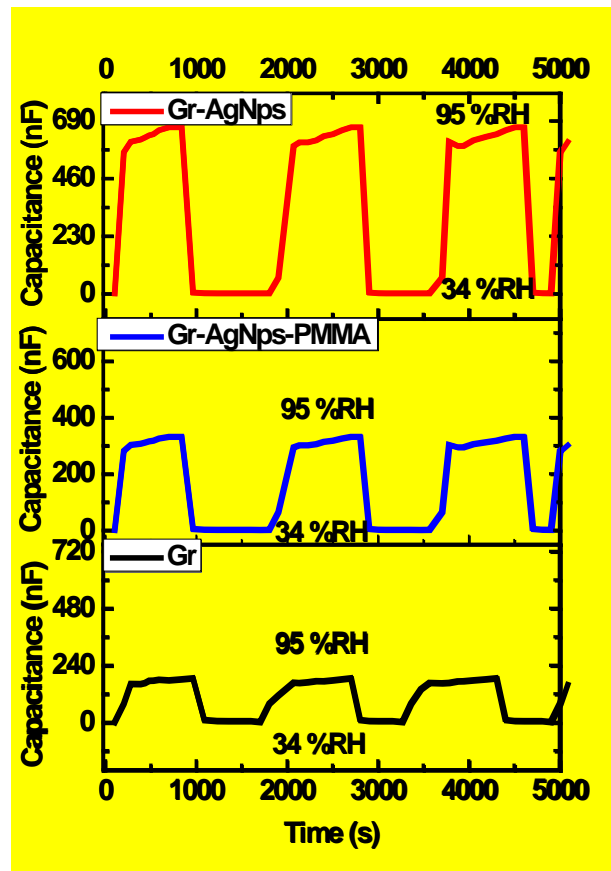
(a)
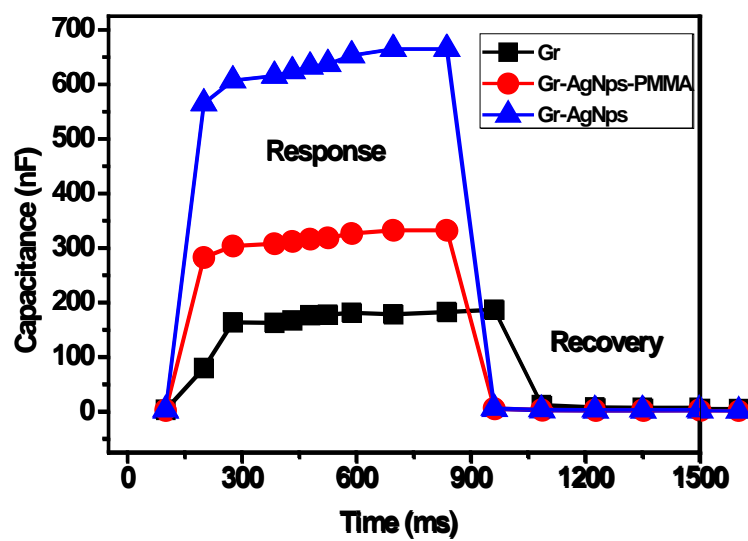
(b)

Figure 9: Response and recovery curve of Gr, Gr-AgNps and Gr-AgNps-PMMA based sensors at 300 K.

Table 1 reports some literature on the calculated response and recovery time for graphene based sensors prepared via various methods. It is obvious from the table that in the present study, we have achieved a faster and sensitive sensor as compared to the earlier reported work.

Table 1: Comparison of various humidity sensor technologies with respect to reported % RH ranges, response and recovery times.

	Material and method	Type	Measured Humidity (%RH)	Response time (s)	Recovery time (s)
Present work	Graphene composites (drop casting)	Capacitive/resistive	97	10 and 12	6
Yao [19]	Graphene oxide	Piezo.	88	19	10
Bi [37]	Graphene oxide	Capacitive	80	10.5	41
Hwang [38]	Graphene (thermal exfoliation)	Resistive	80	180	180
Gosh [39]	Graphene (CVD)	Resistive	63	Not calculated	Not calculated

Hysteresis is one of the shortcomings of an efficient sensor during absorption and desorption. The formation of water clusters in the absorbing surface and the pore geometry is responsible for the occurrence of the hysteresis [40]. Figure 10(a) displays the capacitive hysteresis characteristics during the absorption and desorption of water vapours by increasing the humidity from 40 %RH to 98 %RH and consequently decreasing to 40 %RH for Gr-AgNps

sensors. Both the sensors showed a lagging behind of RH decreasing response from the RH increasing response clearly seen in the figure. Gr-AgNps based sensors shows a lesser hysteresis loss as compared to Gr-AgNps-PMMA based sensor shown in figure 10(b). The hysteresis loss can be reduced and the sensitivity of the device can be made better by using multilayer structure of graphene [41]. The hysteresis calculated for Gr-AgNps and Gr-AgNps-PMMA based sensors was 6 % and 9 % respectively.
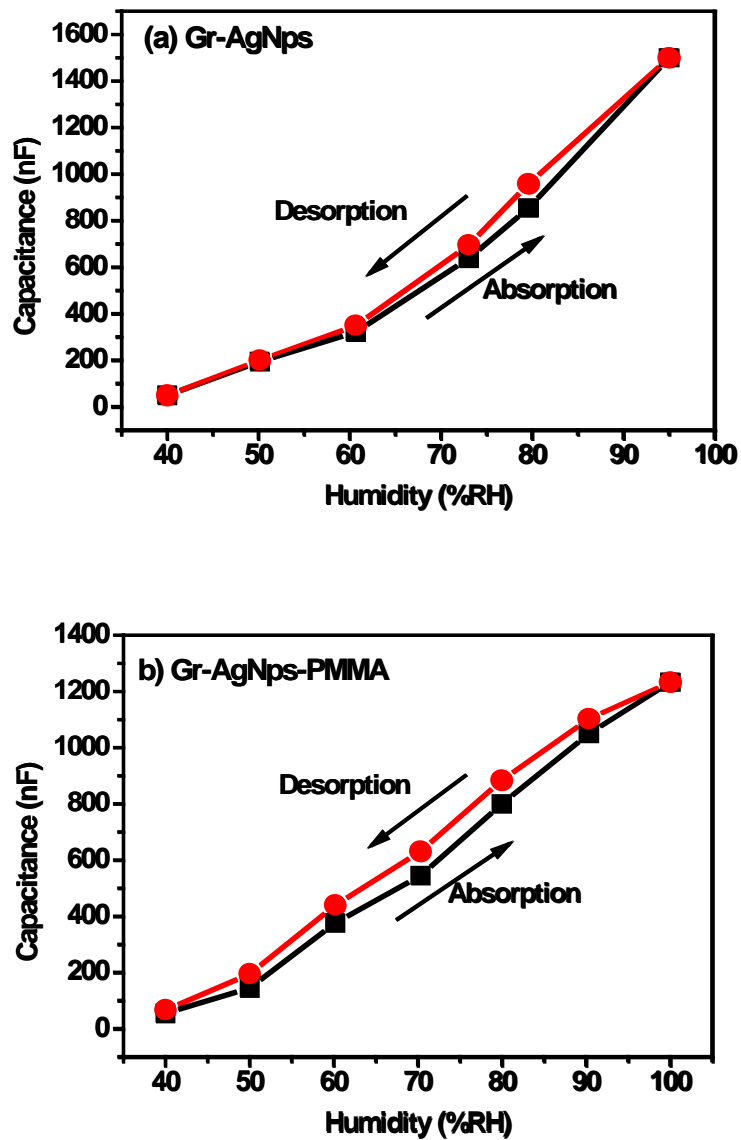

Figure 10: Hysteresis curve of (a) Gr-AgNps(b) Gr-AgNps-PMMA surface type sensor at 300 K.

Figure 11 shows the repeatability of Gr-AgNps and Gr-AgNps-PMMA based sensors performed under the same experimental conditions. The repeatability characteristics is

measured for five exposure cycles repeatedly for 97 %RH. The film humidity sensor exhibited a clear response–recovery behaviour and acceptable repeatability for humidity sensing. the ratio of maximum deviation to full-scale measurement under the same conditions can be termed as the repeatable, and for this study is less than 1 % for both sensors.
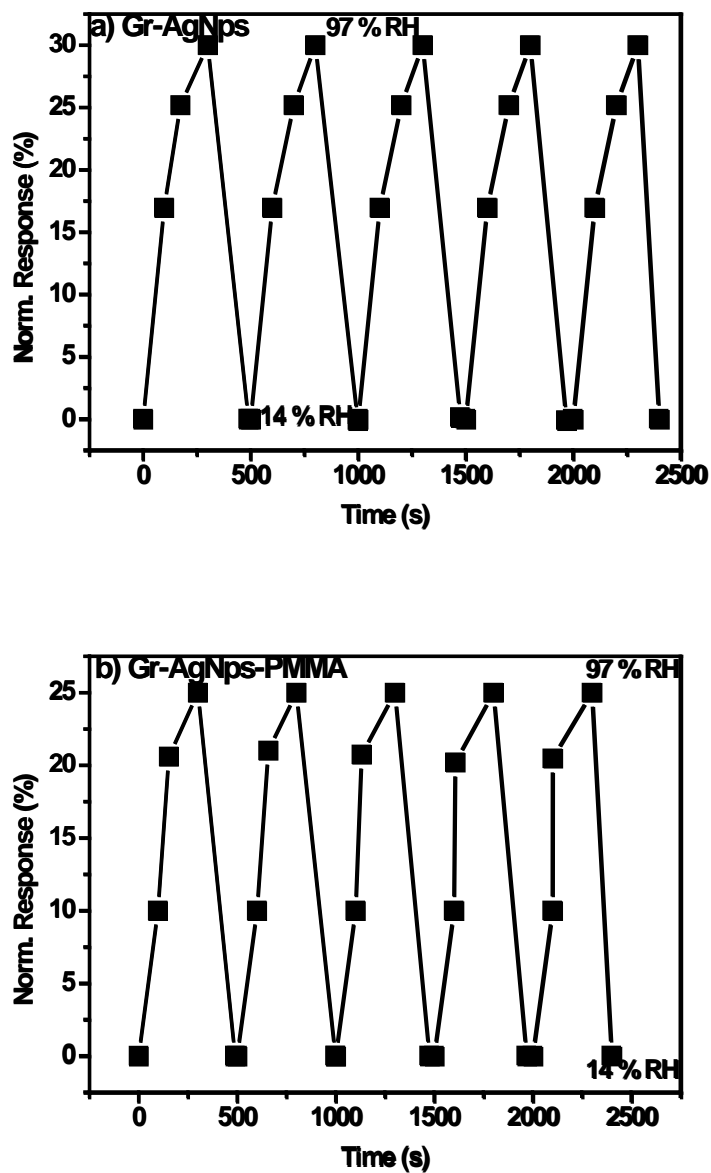

Figure 11: Repeatability of (a) Gr-AgNps(b) Gr-AgNps-PMMA surface type sensor at 300 K.
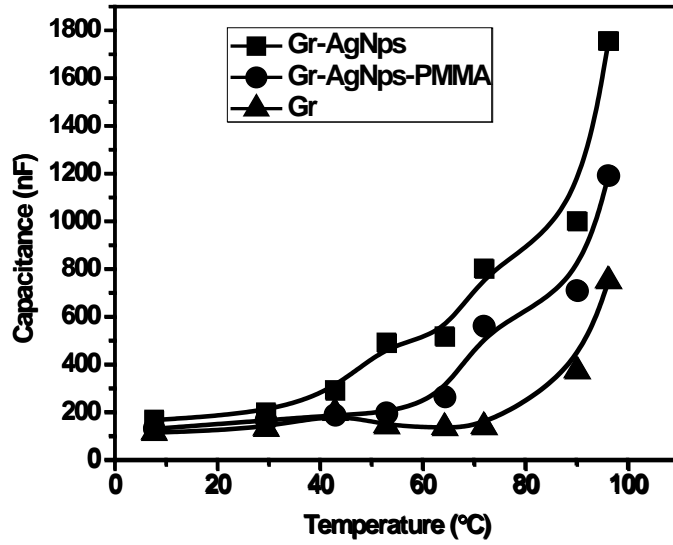
Figure 12: Variation in the capacitance of the sensor with the change in temperature at 45 %RH.

The conduction mechanism in materials is enhanced with the increase in temperature. This may be explained on the basis of percolation theory according to which $\sigma = {}^{1}/_{LZ}$ where σ is the conductivity, Z shows the lowest average resistance of the path and L is the characteristic length, which depends on the concentration of sites. According to this relation increase in temperature increases the average resistance offered by the material which in turn increase the conductivity of the sample material [42, 43]. The decrease in Z is because of generation of charge carriers as a result of increasing temperature [44]. Figure 12 shows the gradual increase in the capacitance of the sensor as the temperature of the surrounding is increased. The increase in the capacitance is due to the increase in the charge carrier concentration hence mobility of charges [45].

2. Conclusions

Simple surface type Gr-AgNps and Gr-AgNps-PMMA thin film based humidity sensors were fabricated via drop casting technique and were investigated. Humidity sensing properties of both the devices were discussed and it was found that Gr-AgNps has better sensing response as compared to Gr-AgNps-PMMA. Addition of AgNps and PMMA to pure graphene successfully induced a small band gap in a zero-band gap material. Due to large effective surface area, the electrical properties of the active layer showed strong dependence on the

frequency. The capacitance of the sensors increased as the humidity is increased due to the change in the dielectric constant. Increase in conductivity hence decrease in resistance has been observed with the increase in the humidity concentration. Both the sensors showed excellent stability and repeatability with complete data consistency for one month. Better response and recovery times are noticed for the Gr-AgNps and Gr-AgNps-PMMA surface based sensors. The hysteresis behaviour of both the sensors were evaluated to be 6 % and 9 % for Gr-AgNps and Gr-AgNps-PMMA thin film based humidity sensors respectively. The temperature treatment has a positive effect on the capacitance of the sensors resulting in the increase in the conductivity keeping the humidity level constant at 45 %RH. Both the sensors showed exciting and efficient performance as humidity sensors and are easy to fabricate and cost effective.

References

1. Fraden, J., Handbook of modern sensors. **2010**.
2. Wei, J.; Zang, Z.; Zhang, Y.; Wang, M.; Du, J.; Tang, X., Enhanced performance of light-controlled conductive switching in hybrid cuprous oxide/reduced graphene oxide (Cu 2 O/rGO) nanocomposites. *Optics letters* **2017,** 42, (5), 911-914.
3. Huang, J.; Hao, Y.; Lin, H.; Zhang, D.; Song, J.; Zhou, D., Preparation and characteristic of the thermistor materials in the thick-film integrated temperature–humidity sensor. *Materials Science and Engineering: B* **2003,** 99, (1), 523-526.
4. Mahadeva, S. K.; Yun, S.; Kim, J., Flexible humidity and temperature sensor based on cellulose–polypyrrole nanocomposite. *Sensors and Actuators A: Physical* **2011,** 165, (2), 194-199.
5. Park, S.; Kang, J.; Park, J.; Mun, S., One-bodied humidity and temperature sensor having advanced linearity at low and high relative humidity range. *Sensors and Actuators B: Chemical* **2001,** 76, (1), 322-326.
6. Lee, C.-Y.; Lee, G.-B., Humidity sensors: a review. *Sensor Letters* **2005,** 3, (1-1), 1-15.
7. Chen, C.-C.; Aykol, M.; Chang, C.-C.; Levi, A.; Cronin, S. B., Graphene-silicon Schottky diodes. *Nano letters* **2011,** 11, (5), 1863-1867.

8.   Kim, Y.; Jung, B.; Lee, H.; Kim, H.; Lee, K.; Park, H., Capacitive humidity sensor design based on anodic aluminum oxide. *Sensors and Actuators B: Chemical* **2009,** 141, (2), 441-446.

9.   Demir, R.; Okur, S.; Şeker, M. e., Electrical characterization of CdS nanoparticles for humidity sensing applications. *Industrial & Engineering Chemistry Research* **2012,** 51, (8), 3309-3313.

10.   Kuang, Q.; Lao, C.; Wang, Z. L.; Xie, Z.; Zheng, L., High-sensitivity humidity sensor based on a single SnO2 nanowire. *Journal of the American Chemical Society* **2007,** 129, (19), 6070-6071.

11.   Zhang, Y.; Yu, K.; Jiang, D.; Zhu, Z.; Geng, H.; Luo, L., Zinc oxide nanorod and nanowire for humidity sensor. *Applied Surface Science* **2005,** 242, (1), 212-217.

12.   Zang, Z.; Zeng, X.; Wang, M.; Hu, W.; Liu, C.; Tang, X., Tunable photoluminescence of water-soluble AgInZnS–graphene oxide (GO) nanocomposites and their application in-vivo bioimaging. *Sensors and Actuators B: Chemical* **2017,** 252, 1179-1186.

13.   Bi, H.; Yin, K.; Xie, X.; Ji, J.; Wan, S.; Sun, L.; Terrones, M.; Dresselhaus, M. S., Ultrahigh humidity sensitivity of graphene oxide. *Scientific reports* **2013,** 3, 2714.

14.   Pearce, R.; Iakimov, T.; Andersson, M.; Hultman, L.; Spetz, A. L.; Yakimova, R., Epitaxially grown graphene based gas sensors for ultra sensitive NO 2 detection. *Sensors and Actuators B: Chemical* **2011,** 155, (2), 451-455.

15.   Zhang, D.; Tong, J.; Xia, B., Humidity-sensing properties of chemically reduced graphene oxide/polymer nanocomposite film sensor based on layer-by-layer nano self-assembly. *Sensors and Actuators B: Chemical* **2014,** 197, 66-72.

16.   Balasubramanian, K.; Burghard, M., Chemically functionalized carbon nanotubes. *Small* **2005,** 1, (2), 180-192.

17.   A., Z. H.; M., A. V., Sensitivity of garphene humidity sensors. *Sensors* **2015,** 10, (1).

18.   Guo, L.; Jiang, H.-B.; Shao, R.-Q.; Zhang, Y.-L.; Xie, S.-Y.; Wang, J.-N.; Li, X.-B.; Jiang, F.; Chen, Q.-D.; Zhang, T., Two-beam-laser interference mediated reduction, patterning and nanostructuring of graphene oxide for the production of a flexible humidity sensing device. *Carbon* **2012,** 50, (4), 1667-1673.

19.   Yao, Y.; Chen, X.; Guo, H.; Wu, Z.; Li, X., Humidity sensing behaviors of graphene oxide-silicon bi-layer flexible structure. *Sensors and Actuators B: Chemical* **2012,** 161, (1), 1053-1058.

20.   Jagtap, S.; Rane, S.; Arbuj, S.; Rane, S.; Gosavi, S., Optical fiber based humidity sensor using Ag decorated ZnO nanorods. *Microelectronic Engineering* **2018,** 187, 1-5.

21.   Choudhury, A., Polyaniline/silver nanocomposites: Dielectric properties and ethanol vapour sensitivity. *Sensors and Actuators B: Chemical* **2009,** 138, (1), 318-325.

22.   Su, P.-G.; Sun, Y.-L.; Lin, C.-C., Humidity sensor based on PMMA simultaneously doped with two different salts. *Sensors and Actuators B: Chemical* **2006,** 113, (2), 883-886.

23.   Humers, W.; Offeman, R., Preparation of graphitic oxide [J]. *J Am Chem Soc* **1958,** 80, (6), 1339.

24.   Geng, W.; Wang, R.; Li, X.; Zou, Y.; Zhang, T.; Tu, J.; He, Y.; Li, N., Humidity sensitive property of Li-doped mesoporous silica SBA-15. *Sensors and Actuators B: Chemical* **2007,** 127, (2), 323-329.

25.   ur Rehman, F.; Tahir, M.; Hameed, S.; Wahab, F.; Aziz, F.; Khalid, F.; Khalid, M. N.; Ali, W., Investigating sensing properties of poly-(dioctylfluorene) based planar sensor. *Materials Science in Semiconductor Processing* **2015,** 39, 355-361.

26.   Rittersma, Z., Recent achievements in miniaturised humidity sensors—a review of transduction techniques. *Sensors and Actuators A: Physical* **2002,** 96, (2), 196-210.

27.   Björkqvist, M.; Salonen, J.; Paski, J.; Laine, E., Characterization of thermally carbonized porous silicon humidity sensor. *Sensors and Actuators A: Physical* **2004,** 112, (2), 244-247.

28.   Omar, M. A., *Elementary solid state physics: principles and applications*. Pearson Education India: 1975.

29.   Ahmad, Z.; Sayyad, M.; Saleem, M.; Karimov, K. S.; Shah, M., Humidity-dependent characteristics of methyl-red thin film-based Ag/methyl-red/Ag surface-type cell. *Physica E: Low-dimensional Systems and Nanostructures* **2008,** 41, (1), 18-22.

30.   Thiwawong, T.; Onlaor, K.; Tunhoo, B., A humidity sensor based on silver nanoparticles thin film prepared by electrostatic spray deposition process. *Advances in Materials Science and Engineering* **2013,** 2013.

31.   Guemart, N.; Bellel, A.; Sahli, S.; Segui, Y.; Raynaud, P., Electrical and structural characterisation of plasma-polymerized TEOS thin films as humidity sensors. *MJ Condensed Matter* **2010,** 12, 208-212.

32.   Kotnala, R.; Shah, J.; Gupta, R., Colossal humidoresistance in ceria added magnesium ferrite thin film by pulsed laser deposition. *Sensors and Actuators B: Chemical* **2013,** 181, 402-409.

33.   Mitra, C.; Ram, S.; Venimadhav, A., Temperature dependent magnetic and dielectric properties of M-type hexagonal BaFe 12 O 19 nanoparticles. *Journal of Alloys and Compounds* **2012,** 545, 225-230.

34.   Zhao, J.; Liu, Y.; Li, X.; Lu, G.; You, L.; Liang, X.; Liu, F.; Zhang, T.; Du, Y., Highly sensitive humidity sensor based on high surface area mesoporous LaFeO 3 prepared by a nanocasting route. *Sensors and Actuators B: Chemical* **2013,** 181, 802-809.

35.   Gao, W.; Singh, N.; Song, L.; Liu, Z.; Reddy, A. L. M.; Ci, L.; Vajtai, R.; Zhang, Q.; Wei, B.; Ajayan, P. M., Direct laser writing of micro-supercapacitors on hydrated graphite oxide films. *Nature Nanotechnology* **2011,** 6, (8), 496-500.

36.   Zhang, D.; Chang, H.; Li, P.; Liu, R.; Xue, Q., Fabrication and characterization of an ultrasensitive humidity sensor based on metal oxide/graphene hybrid nanocomposite. *Sensors and Actuators B: Chemical* **2016,** 225, 233-240.

37.   Bi, H.; Yin, K.; Xie, X.; Ji, J.; Wan, S.; Sun, L.; Terrones, M.; Dresselhaus, M. S., Ultrahigh humidity sensitivity of graphene oxide. *Scientific reports* **2013,** 3.

38.   Smith, A. D.; Elgammal, K.; Niklaus, F.; Delin, A.; Fischer, A. C.; Vaziri, S.; Forsberg, F.; Råsander, M.; Hugosson, H.; Bergqvist, L., Resistive graphene humidity sensors with rapid and direct electrical readout. *Nanoscale* **2015,** 7, (45), 19099-19109.

39.   Ghosh, A.; Late, D. J.; Panchakarla, L.; Govindaraj, A.; Rao, C., NO2 and humidity sensing characteristics of few-layer graphenes. *Journal of Experimental Nanoscience* **2009,** 4, (4), 313-322.

40.   Sakai, Y.; Sadaoka, Y.; Matsuguchi, M., Humidity sensors based on polymer thin films. *Sensors and Actuators B: Chemical* **1996,** 35, (1-3), 85-90.

41.   Li, Y.; Yang, M., Bilayer thin film humidity sensors based on sodium polystyrenesulfonate and substituted polyacetylenes. *Sensors and Actuators B: Chemical* **2002,** 87, (1), 184-189.

42.   Böttger, H.; Bryksin, V., Hopping Conduction in Solids (VCH, Deerfield Beach, FL). **1985**.

43.   Dyakonov, V.; Sariciftci, N., Organic photovoltaics: concepts and realization. In Springer, New York: 2003.

44.   Hsueh, H.; Hsueh, T.; Chang, S.; Hung, F.; Tsai, T.; Weng, W.; Hsu, C.; Dai, B., CuO nanowire-based humidity sensors prepared on glass substrate. *Sensors and Actuators B: Chemical* **2011,** 156, (2), 906-911.

45.   Tahir, M.; Hassan Sayyad, M.; Wahab, F.; Ahmad Khalid, F.; Aziz, F.; Naeem, S.; Naeem Khalid, M., Enhancement in the sensing properties of methyl orange thin film by TiO 2 nanoparticles. *International Journal of Modern Physics B* **2014,** 28, (05), 1450032.